

Computer Simulation and Tank Experimental Verification of Concentric Ring Electrodes

W. Besio¹, K. Koka¹, R. Patwardhan²

¹Department of Biomedical engineering, Louisiana Tech University-Ruston, LA, USA

²Department of Neurosurgery, Louisiana State University-Shreveport, LA, USA

Abstract—Brain activity generates electrical potentials that are spatio-temporal in nature. EEG is the least costly and most widely used non-invasive technique for diagnosing many problems related to the brain. It has very good temporal resolution, but does not pose high spatial resolution primarily due to the blurring effects of the volume conductor. The surface Laplacian enhances the spatial resolution and selectivity of the surface electrical activity as it takes the second spatial derivative of the potential.

In an attempt to increase the localization and spatial selectivity a five point finite difference method has recently been used in a bipolar electrode configuration. Here we report on a nine point finite difference method as a model for the tripolar electrode configuration.

We have designed a computer simulation to model electrode properties and a dipole at various depths below the electrode surface. A tank experimental was setup to verify the computer simulated potentials. In the simulation and tank experiment, a concentric ring electrode of 2cm diameter was used.

We found that the tripolar electrode configuration has significantly better localization and signal to noise ratio than the bipolar and quasi-bipolar configurations.

Keywords—Electroencephalography, EEG, surface Laplacian, spatial selectivity, five point method, nine point method, quasi-bipolar and tripolar.

I. INTRODUCTION

The potentials measured from the brain electrical activity by functional magnetic resonance imaging (fMRI) and positron emission tomography (PET) have low temporal resolution, taking hundreds of milliseconds to acquire necessary signals to form images. Electroencephalography (EEG) systems are much faster requiring only a few milliseconds for mapping scalp surface activity. According to Srinivasan [1], since the skull is such a poor conductor, current flow in the skull will mostly be radial, flowing from the inner to outer surface of the skull. This being the case, any magnetic system that detects tangential sources such as MEG will have problems resolving sources in the brain. In addition, fMRI, PET and MEG are all costly and not portable. EEG systems have the high temporal resolution necessary to produce movie like images of the scalp surface potentials as the brain activities change.

II. BACKGROUND

Brain activity is a spatio-temporal phenomenon. It is distributed throughout the brain at different times. Ions are associated with this action and their flow creates electrical activity that can be detected on the scalp surface with EEG instrumentation. Hans Berger recorded the first human EEG from the scalp in 1924. Today, EEG still is and will continue to be a most important non-invasive method for investigating the activity of the brain. Of the methods for recording brain activity, EEG is the cheapest and gives sufficient temporal resolution to study the functioning of the brain.

Much advancement has come recently in the field of EEG, making it even more appealing for brain activity analysis. One such advancement is the application of surface Laplacian to EEG. Surface Laplacian mapping has been shown to enhance the high spatial frequency components and spatial selectivity of the electrical activity located close to the observation point [2-3]. These unique characteristics are based on the surface Laplacian being the second spatial derivative of the potential.

The application of Laplacian to EEG started with Hjorth [4] utilizing a five-point difference method. Many other approaches have revealed positive results as well, estimating the scalp Laplacian from the potential EEG measurements. Such approaches include the spline Laplacian algorithm by Perrin [5], and ellipsoidal spline Laplacian algorithm by Law and realistic geometry Laplacian algorithms. He [2-3] calculated the surface Laplacian with Hjorth's [4] technique from an array of five disc sensors measuring surface potentials, but these discs accept global signals and may be directionally dependent as suggested by Geselowitz and Ferrara [6].

In this paper, we discuss the computer modeling of the concentric ring electrode and the verification with data collected from tank experiments. Three electrode systems were tested: bipolar electrode, quasi-bipolar electrode [7-9] and tripolar electrode. Results are given for 2cm diameter outer ring electrodes.

III. METHODOLOGY

A. Bipolar electrode:

The bipolar electrode consists of a disc surrounded by a ring and is illustrated in Fig.1. For comparison, the sizes of the bipolar electrode elements are kept equal to that of the outer ring of the other electrode element configurations.

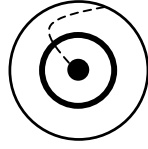


Fig.1. For the bipolar configuration the disc and outer ring are used. For the quasi-bipolar configuration, the disc and outer ring are shorted. In the tripolar configuration, all three elements are independently used.

If we apply the five-point difference method of Hjorth [3], to a disc and concentric ring by taking the integral along a circle of radius r from the center of the disc and defining $X=r \text{Cos}(\theta)$, $Y=r \text{Sin}(\theta)$ the Laplacian Δv_0 for the bipolar electrode system [10] can be given as

$$\Delta v_0 \cong \frac{4}{(2r)^2} (\bar{v} - v_d) \quad (1)$$

Where \bar{v} is the voltage on the outer ring and v_d is the voltage at the center of an electrode with radius r .

B. Quasi-Bipolar electrode:

In the quasi-bipolar configuration, the electrode has three elements (disc, middle ring and an outer ring). It is called quasi-bipolar because the disc and outer ring are shorted. The Laplacian potential for the quasi-bipolar electrode configuration is given as [6-9]

$$\Delta v_o = \frac{(\bar{v} + v_d)}{2} - v_m \quad (2)$$

Here \bar{v} is the voltage on the outer ring, v_m is the voltage on the middle ring and v_d is the voltage on the disc.

C. Tri polar electrode:

It consists of a disc surrounded by two concentric rings. The tripolar electrode is designed based on our unpublished Nine-point method, which is similar to methods used in image processing. In this configuration the Laplacian potential for the tripolar electrode is given by

$$\Delta v_0 \cong \frac{1}{3r^2} \{16(v_m - v_d) - (\bar{v} - v_d)\} \quad (3)$$

Here r is the radius between each electrode element and \bar{v} is the voltage on the outer ring, v_m is the voltage on the middle ring and v_d is the voltage on the disc.

D. Computer Simulation:

A mathematical model patterned after Fig. 2, is designed using the analytical solution (4) to calculate the potential due to a dipole with given conductivity σ

$$V = \frac{1}{4\pi\sigma} \cdot \frac{(\bar{r}_p - \bar{r}) \cdot \bar{P}}{|\bar{r}_p - \bar{r}|^3} \quad (4)$$

In this mathematical model $(1/4\pi\sigma)$ is taken as a constant, pertaining to the conductivity of salt water and the permittivity of the PCB material used for the dipole preparation. These values are discussed further in the results section.

For the simulation, the outer concentric ring electrodes range from 0.5 to 3.0cm in diameter with the disc and middle ring sized proportionally. An axial dipole, directed towards the positive Z-axis, is moved incrementally 1.0cm at a time in the Z-axis from depths of 1.0cm to 4.0cm. The dipole traverses the X-axis from -5.0cm to 5.0cm and in the Y-axis from -5.0cm to 5.0cm . The depth of the dipole is kept constant while moved in the X-Y plane along the different lines. Then the depth of the dipole is changed and it is moved in the X-Y plane again. From the simulated model of the moving dipole, the potential values on each electrode element are calculated using the analytical formula (4). These potentials are then used to calculate the Laplacian of the: bipolar electrode by (1), the quasi-bipolar electrode by (2), and the tripolar electrode with (3).

From the calculated Laplacian for the bipolar, quasi-bipolar, and tripolar electrode configurations, the attenuation in dB of the signal along the radial direction is calculated and plotted.

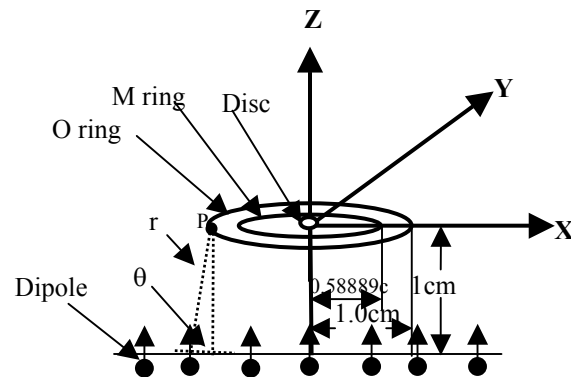


Fig.2. Concentric ring electrode configuration for the moving dipole computer simulation. The disc in the center is surrounded by concentric rings. The dipole directed in the positive Z axis is moved incrementally 1.0cm at a time from -1.0cm to -4.0cm . The dipole is moved left to right from -5.0cm to 5.0cm along the X axis. The middle ring is used for the quasi-tripolar and tripolar electrode configurations.

E. Tank Experiment:

In order to validate the results obtained by the computer simulation, tank experiments are conducted. A tank of Plexi-Glass with sizes 50cm X 26cm X 30cm is used. This tank is filled with a saltwater mix of 9gm/L concentration. The dipole is prepared with two thin copper discs etched on a two-sided PC board opposite to each other. A 5V pk-pk, 100Hz square wave is applied between the discs. The two discs are given opposite polarity square waves. To limit the corrosion of dipole discs, the 100Hz square wave is applied instead of a DC source.

The concentric electrodes were designed with ORCAD software and prepared using the LPKF ProtoMat[®] C20 rapid prototype board plotter. The concentric ring electrode was attached to a lead screw driven stage and moved along the X-axis at the rate of 1.8cm/sec. The depth was kept constant for each of five passes of the stage with the measurements averaged to minimize the variations. Then the depth was changed and the measurements were taken until all depths were completed.

Potential measurements are taken on the three elements of the concentric ring electrodes using a custom LabView program via a National Instruments DaqCard 700. The measurements are referenced by an electrode between the dipole discs. Post processing is achieved with a custom Matlab program. Laplacian potentials are calculated for all three configurations of electrodes using the formulae (1) – (3). The attenuation of the signal along the radial distance is calculated and dB attenuation is plotted for comparison between the three electrode configurations.

The signal to noise ratio (SNR) was calculated for the three configurations. This was calculated by dividing the peak value of the signal by the peak value of the base line, which is assumed noise. This was done for 6 recordings. Two sample t-test, assuming unequal variance were conducted on the SNRs to compare the performance between the different electrode configurations.

IV. RESULTS

Calculation of Laplacian potential and localization effect for three concentric electrode configurations:

For comparison, the sizes of the electrode elements were kept the same between the tank experiments and the computer models. The outer ring was set at 2cm diameter for all. The middle ring used in the quasi-bipolar and tripolar configuration was 1.18cm diameter, and the disc had a diameter of 0.14cm. The width of the ring was 0.03cm and the depth of the dipole was 1.0cm below the surface. In the tank experiments electrodes were moved in the X-direction on the surface of the saltwater solution and the dipole was stationary at $y = 0.0\text{cm}$. The potential measurements were taken for only one Y value, which is different from the computer simulation. Laplacian potentials for bipolar, quasi-

bipolar and tripolar configurations were then calculated using the respected formulae. These are plotted in Fig.3 (Panels A to C). The attenuation of the potential for these three configurations along the radial distance was calculated for a 2cm diameter electrode. These curves are plotted together in Fig.3 (panel D). The attenuation values are plotted in dB.

The nine point method (tripolar configuration) was significantly better at the 1% confidence level with steeper attenuation compared to the other two electrode configurations.

Validation of simulated data with the measured data:

In Fig.4, the attenuation in dB for the three configurations, quasi-bipolar, bipolar and tripolar from the simulated data are compared with the measured tank experimental data of each configuration. The attenuation in dB along the radial distance is plotted in three individual panels of Fig.4 for the three electrode configurations.

The calculated SNRs for the measured data from the tank experiment for three configurations are given as: quasi bipolar-16.5, bipolar-6.25 and tripolar-16.9. The tripolar configuration SNR was significantly better at the 1% confidence level compared to the other electrode configurations.

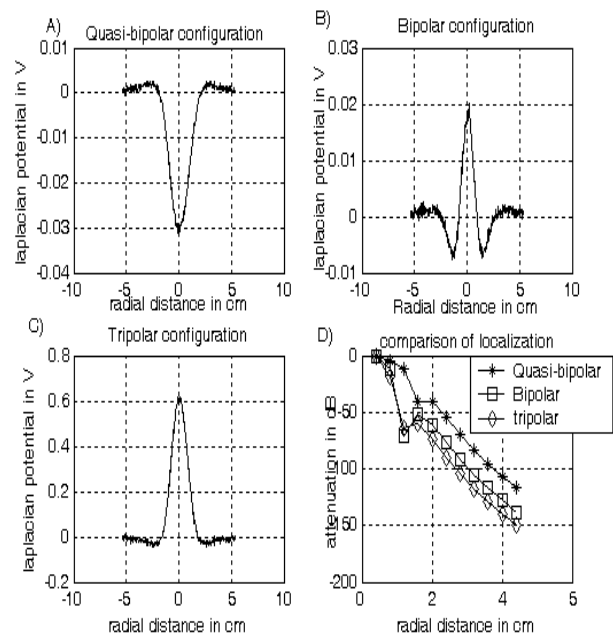


Fig.3. Laplacian potentials measured from the tank experiment for (A) quasi bipolar, (B) bipolar and (C) tripolar. Panel (D) shows the attenuation in dB for the three configurations.

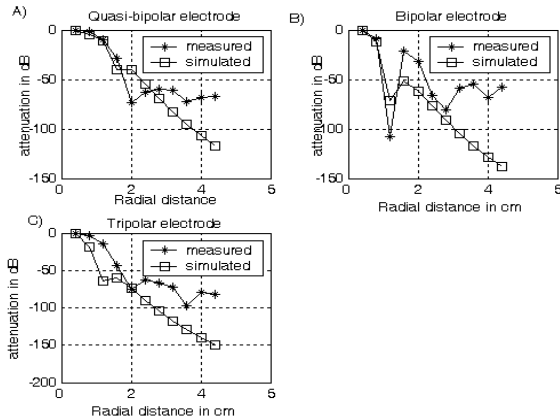


Fig.4. Comparison of measured attenuation in dB with the simulated attenuation of laplacian potentials. Panel (A) quasi-bipolar configuration, panel (B) bipolar configuration, and panel (C) tripolar configuration.

V. DISCUSSION

From the measured tank experimental data and the simulated data, for the 2cm diameter concentric electrode it was determined that the tripolar electrode has more localization capacity than the other two electrode configurations. This can be seen from Fig.3, the tripolar graph, shown with diamonds, is the bottom curve. This means that the attenuation is greatest for the tripolar electrode configuration for distant sources. It also shows that the tripolar electrode configuration is more sensitive to the local signals than the other configurations. The statistical analysis also verified there was a significant difference between the tripolar configuration and the others.

In Fig.4, it can be seen that the shape of the attenuation of the Laplacian potential for the three configurations in the computer simulated data are very similar to the measured data from the tank experiment. There is a slight difference between the simulated and measured values. This can be justified by a scaling factor, which comes from negligence in the computer simulation of conductivity for saltwater and permittivity of the PCB material used in between the two thin discs of copper used to form the dipole. In the tank experiments there are also noise sources which contaminate our signals.

V. CONCLUSION

The attenuation of the tripolar electrode configuration is significantly better than the other two configurations tested in this study. This property will be beneficial in localizing sources that could be used in imaging. The SNR improvement over existing configurations is also a positive attribute that will enhance our mapping capabilities. Further work is needed to test more electrodes with different diameters and dipoles at different depths.

ACKNOWLEDGMENT

We would like to thank the Louisiana Tech Center for Entrepreneurship and Information Technology (CEIT), The Louisiana Board of Regents (grant# LEQSF(2003-05)-RD-B-05) and all of our lab members for their help.

REFERENCES

- [1] Srinivasan R, Methods to Improve the Spatial Resolution of EEG, *J Bioelectromagnetism* vol. 1, pp. 102-111, 1999.
- [2] He B, *Brain Electrical Source Imaging: Scalp Laplacian Mapping and Cortical Imaging*, *Crit Rev Biomed Eng*, vol. 27, pp. 149-188, 1999.
- [3] He B., Lian J., and Li G.; *High-resolution EEG: a new realistic geometry spline Laplacian estimation technique*; *Clin. Neurophysiology* 112, pp 845-852, 2001.
- [4] Hjorth B., *An On-Line Transformation of EEG Scalp Potentials into Orthogonal Source Derivations*, *EEG and Clin. Neurophysiology*, 39, pp. 526-530, 1975.
- [5] Perrin F, Bertrand O, and Pernier J, *Scalp Current Density Mapping: Value and Estimation from Potential Data*; *IEEE Trans Biomed Eng*, vol. 34, pp. 283-288, 1987.
- [6] Geselowitz D. and Ferrara J., *Is Accurate Recording of the ECG Surface Laplacian Feasible?* *IEEE Trans. BME*, 46(4), pp. 377-381, 1999.
- [7] Besio W. and Tarjan P., *Atrial Activation Pattern from Surface Laplacian Electrocardiograms of Humans*, *International Journal of Bioelectromagnetism*, vol. 4, pp. 95-96, 2002.
- [8] Besio W. and Tarjan P., *Filtering of Surface Laplacian Electrocardiograms From Humans to Produce Atrial Activation Patterns*, *Proceedings of 24th Annual International Conference of the IEEE EMBS and the 2002 Fall Meeting of the BMES*.
- [9] Besio W., Lu C. and Tarjan P., *A Feasibility Study for Body Surface Cardiac Propagation Maps of Humans from Laplacian Moments of Activation*, *Electromagnetics*, vol. 21, pp. 621-632, 2001.
- [10] Leon Lapidus and Geroge F. Pinder, *Numerical solution of partial differential equations in science and engineering*, John Wiley & Sons, 1982, pp.371-372.
- [11] Van Oosterom A, and Strackee J, *Computing the Lead Field of Electrodes with Axial Symmetry*, *Medical & Biological Engineering & Computing*. (21), pp. 473-481, 1983
- [12] Bradshaw L and Wikswo J, *Spatial Filter Approach for Evaluation of the Surface Laplacian of the Electroencephalogram and Magnetoencephalogram*, *Ann BME* vol. 29, pp. 202-213, 2001.